

# **Infrared Spectroscopy of NaCl(CH<sub>3</sub>OH)<sub>n</sub> Complexes in Helium Nanodroplets**

Ahmed M. Sadoon,<sup>1,2</sup> Gautam Sarma,<sup>1</sup> Ethan M. Cunningham,<sup>1</sup> Jon Tandy,<sup>1</sup> Magnus W. D.  
Hanson-Heine,<sup>3</sup> Nicholas A. Besley,<sup>3</sup> Shengfu Yang<sup>1\*</sup> and Andrew M. Ellis<sup>1\*</sup>

<sup>1</sup>Department of Chemistry, University of Leicester, University Road, Leicester, LE1 7RH,  
UK

<sup>2</sup>Department of Chemistry, College for Pure Sciences, University of Mosul, Iraq

<sup>3</sup>School of Chemistry, University of Nottingham, University Park, Nottingham NG7 2RD,  
UK

Email: [sfy1@le.ac.uk](mailto:sfy1@le.ac.uk); [andrew.ellis@le.ac.uk](mailto:andrew.ellis@le.ac.uk)

Tel. +44 116 252 2138

---

Manuscript submitted to *Journal of Physical Chemistry A*

## **Abstract**

Infrared (IR) spectra of complexes between NaCl and methanol have been recorded for the first time. These complexes were formed in liquid helium nanodroplets by consecutive pick-up of NaCl and CH<sub>3</sub>OH molecules. For the smallest NaCl(CH<sub>3</sub>OH)<sub>*n*</sub> complexes where *n* = 1-3, the IR data suggest that the lowest energy isomer is the primary product in each case. The predominant contribution to the binding comes from ionic hydrogen bonds between the OH in each methanol molecule and the chloride ion in the NaCl, as established by the large red-shift of the OH stretching bands compared with the isolated CH<sub>3</sub>OH molecule. For *n* ≥ 4 there is a dramatic shift from discrete vibrational bands to very broad absorption envelopes, suggesting a profound change in the structural landscape and, in particular, access to multiple low-energy isomers.

## Introduction

Alkali halides (MX) are the archetypal univalent salts. The crystalline structure of the solid is disrupted by water and these salts readily dissolve to form separated ions in dilute aqueous solutions. If the solid represents one extreme, then the counterpart is an isolated MX molecule. How might this smallest entity of salt, a single MX molecule, behave in the presence of a small water cluster,  $(\text{H}_2\text{O})_n$ ? This problem can be addressed in experiments by forming isolated  $\text{MX}(\text{H}_2\text{O})_n$  complexes and then using techniques, such as spectroscopy, to determine their properties. Such studies offer insight into the interaction between the constituent ionic particles and the solvent, and can be reinforced through quantum chemical calculations. Understanding these interactions and the balance between them is critical in being able to carry out accurate simulations of bulk solutions.<sup>1</sup>

An early infrared spectroscopic study of an NaCl/H<sub>2</sub>O mixture in an argon matrix provided a tentative assignment of vibrational bands of the NaCl(H<sub>2</sub>O) complex.<sup>2</sup> The first detailed spectroscopic study of several different NaCl(H<sub>2</sub>O)<sub>n</sub> complexes ( $n = 1-3$ ) was obtained by microwave spectroscopy and this revealed important structural information.<sup>3,4</sup> We have recently shown that complexes between NaCl and water molecules can be formed inside liquid helium nanodroplets and this made it possible to record the first infrared (IR) spectra of several small NaCl(H<sub>2</sub>O)<sub>n</sub> complexes.<sup>5</sup> The spectra for  $n = 1-3$  are consistent with structures in which an ionic hydrogen bond (IHB) is formed between a single OH group in each water molecule and the Cl<sup>-</sup> in the salt. Evidence for inter-water hydrogen bonding only begins to appear for  $n \geq 4$ .

An alternative solvent to water is methanol. Most solid alkali halides will dissolve in methanol but their solubility is far lower than in water.<sup>6,7</sup> The reduced solubility of salts in methanol when compared with water is a consequence of the hydrophobic (CH<sub>3</sub>) group in the former. It would therefore be interesting to investigate how this amphiphilic character affects

the interactions between a single salt molecule and one or more methanol molecules. It is well-known that addition of a salt to bulk water/alcohol mixtures causes a “salting-out” effect,<sup>8</sup> in which the salt induces aggregation of the alcohol molecules and can bring about a phase separation into an aqueous salt phase and an alcohol/water phase. This phenomenon has some similarities to the salting-out effect associated with protein solubility in the Hofmeister series.<sup>9</sup> There has been some controversy about how this phase separation happens. On the basis of neutron scattering measurements on NaCl in *t*-butanol, Bowron and Finney proposed that the salting-out effect is driven by a salt bridge consisting of a halide ion linking two alcohol molecules through two ionic hydrogen bonds.<sup>10</sup> However, Paschek *et al.* have rejected this suggestion and have instead presented both experimental and theoretical evidence for an alternative mechanism in which a halide ion attaches to the methyl groups in *t*-butanol and thereby enhances the attractive interactions between the hydrophobic methyl groups in different *t*-butanol molecules.<sup>11</sup> These two explanations of the salting-out effect are clearly very different.

As a stepping stone to the study of the solvation of alkali halide molecules by more complex alcohols, as well as alcohol/water mixtures, we describe here the first IR spectroscopic study of NaCl(CH<sub>3</sub>OH)<sub>*n*</sub> complexes. The resulting data are consistent with the formation of contact ion-pair structures in which up to three methanol molecules can bind to an intact NaCl molecule, predominantly via ionic hydrogen bonds between the OH groups and the chloride ion. These structures are analogous to the salt-bridge structures mentioned in the previous paragraph. For larger complexes the narrow spectral bands are replaced with broad absorption features, which seem to arise from contributions from multiple low energy conformers. In tandem with the experimental work we employ quantum chemical calculations to explore the structural landscape of the complexes for  $n \leq 4$ .

## Experimental

Full details of the apparatus and techniques employed here can be found in previous publications.<sup>5,12</sup> In brief, helium nanodroplets with a mean size close to 5000 helium atoms were formed by expanding pre-cooled gaseous helium into a vacuum through a 5  $\mu\text{m}$  pinhole. The droplets then passed through two consecutive pick-up cells, the first containing NaCl vapor and the second methanol vapor. Gaseous NaCl was produced by resistively heating a pick-up cell containing solid sodium chloride. The temperature of this cell (445  $^{\circ}\text{C}$ ) was chosen to ensure that most helium droplets contained no more than one NaCl molecule, as confirmed by recording mass spectra. Mass spectra of NaCl and its clusters in the gas phase have shown that the primary ion from NaCl is  $\text{Na}^+$  whereas that from the  $(\text{NaCl})_2$  dimer is  $\text{Na}_2\text{Cl}^+$ .<sup>13</sup> The NaCl vaporization conditions were therefore adjusted so that the  $\text{Na}_2\text{Cl}^+$  signal detected by electron ionization mass spectrometry was small relative to  $\text{Na}^+$  prior to addition of methanol in the second pick-up cell.

Infrared spectra were recorded via a depletion method which exploits the evaporative loss of helium atoms as the absorbed energy becomes dispersed into the droplet. This effect causes a decrease in the droplet size and therefore its geometric cross section, which can be registered by a drop in the signal identified via electron ionization mass spectrometry downstream of the IR excitation zone. In the current experiments mass-selective ion detection has been used. This is important for two reasons: (1) by choosing appropriate ions we can eliminate any contributions to the IR spectra from pure methanol and its clusters; (2) it provides a degree of size selectivity which aids spectral assignment, as detailed later. The linewidth of the optical parametric oscillator used to excite IR transitions is 4-5  $\text{cm}^{-1}$ .

## Computational details

Calculations on  $\text{NaCl}(\text{CH}_3\text{OH})_n$  for  $n = 1-4$  were carried out using density functional theory (DFT) within the Q-Chem software package.<sup>14</sup> Geometry searches, energy evaluations and vibrational frequency calculations were performed using the M06 functional.<sup>15</sup> In order to search through a wide range of potential geometries, a total of 50 different initial configurations were generated by randomly rotating and translating each molecule within a  $50 a_0^3$  box ( $a_0 =$  the atomic unit of length = 0.5292 Å), with the NaCl bond length fixed at 2.481 Å for  $n = 1$ , 2.607 Å for  $n = 2$ , 2.907 Å for  $n = 3$ , and 3.085 Å for  $n = 4$ , as the length of the NaCl bond is found to lengthen with the addition of extra methanol molecules. In order to avoid self-consistent field convergence problems, atoms in different molecules were prevented from becoming closer than  $3 a_0$  from each other. The initial configurations were then optimized without constraint (including variation of the Na-Cl distance) at the M06/6-31+G(d) level of theory with the default SG-1 integration grid. For the smaller  $n = 1$  and 2 complexes, all structures were re-optimized at the M06/6-311++G(d,p) with an EML-(150,770) integration grid. For the  $n = 3$  and 4 complexes, only the structures within 50 kJ mol<sup>-1</sup> of the minimum energy structure were re-optimized at the higher level of theory.

Harmonic vibrational frequencies were then calculated and scaled to account for anharmonicity. Scaling factors for harmonic frequency calculations are well established but these scaling factors represent an average over many different types of vibrational mode.<sup>16</sup> In this work, we derive a *system-specific* scaling factor for the OH stretching modes of the  $\text{NaCl}(\text{CH}_3\text{OH})_n$  complexes. This scaling factor is derived purely on the basis of reference to anharmonic vibrational frequency calculations, i.e. there is no use of experimental data. The anharmonic frequency calculations were performed using second-order vibrational perturbation theory (VPT2), as well as the using transition optimized shifted Hermite (TOSH) variation on VPT2<sup>17</sup> for the lowest energy  $\text{NaCl}(\text{CH}_3\text{OH})_n$  ( $n = 1$  and 2) complexes. Third- and fourth-order derivatives of the energy with respect to nuclear displacement were

evaluated for up to two-mode couplings. The approach adopted used finite differences and employed analytical gradients produced from a step size of 0.5291 Å along each normal mode. Averaging over the three vibrational modes and two methods gives a scaling factor of 0.924 for  $\text{NaCl}(\text{CH}_3\text{OH})_n$  complexes. This value is lower than standard values for the scaling factor,<sup>16</sup> which suggests that the OH stretching mode in these complexes has a high degree of anharmonicity, which in turn may be a consequence of the ionic hydrogen bonding (see later). A similar analysis for a single methanol molecule gives a value of 0.948, which is closer to the standard values for scaling factors.

## Results and Discussion

### 1. *Overview of the experimental results*

Figure 1 shows an illustrative mass spectrum in which two series of peaks are highlighted, one assigned to  $(\text{CH}_3\text{OH})_m\text{H}^+$  and the other to  $(\text{CH}_3\text{OH})_m\text{Na}^+$ . The  $(\text{CH}_3\text{OH})_m\text{H}^+$  ions derive from ionization of helium droplets containing only methanol clusters, while the  $(\text{CH}_3\text{OH})_m\text{Na}^+$  ions are the products of ionization of helium droplets containing  $\text{NaCl}(\text{CH}_3\text{OH})_n$  complexes, where  $n \geq m$ . We have previously seen loss of Cl atoms from ionization of  $\text{NaCl}(\text{H}_2\text{O})_n$  complexes in helium droplets<sup>5</sup> and a parallel process must occur here for the ionization of  $\text{NaCl}(\text{CH}_3\text{OH})_n$ . To record IR spectra we have monitored the IR-induced depletion of specific  $(\text{CH}_3\text{OH})_m\text{Na}^+$  ions.

Figure 2 shows IR spectra recorded by monitoring the ion signals for  $m = 1-4$ . Bands with relatively narrow linewidths are seen for  $m = 1-3$  in both the OH stretching and CH stretching regions. However, for  $m = 4$  only a very broad OH stretching feature is seen which reaches a maximum near  $3300 \text{ cm}^{-1}$ .

Before attempting to make specific IR band assignments we first discuss the calculated structures for small  $\text{NaCl}(\text{CH}_3\text{OH})_n$  complexes.

## 2. Predicted structures

Four structures corresponding to distinct minima were found for the NaCl(CH<sub>3</sub>OH) complex in the DFT calculations, all of which are shown in Figure 3. In the global minimum, the NaCl ion-pair is oriented so that the chloride ion can form an ionic hydrogen bond (IHB) with the OH, while additional stabilization is gained by the proximity of the Na<sup>+</sup> ion to the O atom. Similar behaviour has been seen previously for NaCl(H<sub>2</sub>O).<sup>4,5</sup> In the next lowest energy minimum, which is 10.7 kJ mol<sup>-1</sup> higher in energy than the global minimum, one of the C-H bonds points towards the chloride ion.

For NaCl(CH<sub>3</sub>OH)<sub>2</sub> we have found five distinct minima (see Figure 4). The lowest energy structure is analogous to the  $n = 1$  complex but now has two IHBs linking the chloride ion and the OH groups. The next lowest energy minimum lies 2.9 kJ mol<sup>-1</sup> above the global minimum and has two distinct bonding modes, one with methanol attached to the NaCl via an IHB. The other methanol molecule in this structure is oriented to allow partial interaction with both the OH group and one of the CH bonds from the methyl group.

For  $n = 3$  and 4 the conformational landscapes are more complex. The global minimum for NaCl(CH<sub>3</sub>OH)<sub>3</sub> is analogous to those found for NaCl(CH<sub>3</sub>OH) and NaCl(CH<sub>3</sub>OH)<sub>2</sub>, but now with three equivalent IHBs (see Figure 5). However, other minima are now more energetically accessible than in the smaller complexes. In the lowest energy structure for NaCl(CH<sub>3</sub>OH)<sub>4</sub> one methanol molecule is no longer bound to NaCl via an ionic hydrogen bond. Instead this methanol is effectively in a second solvation shell and is hydrogen-bonded to one of the methanol molecules in the inner solvation shell (see Figure 6). However, there is a significant increase in the number of low energy structures available for NaCl(CH<sub>3</sub>OH)<sub>4</sub> when compared with NaCl(CH<sub>3</sub>OH)<sub>3</sub>.



### 3. *Assignment of IR spectra: OH stretching*

We start by considering bands in the OH stretching region. Here there are several relatively narrow bands seen in Figures 2(a), (b) and (c) obtained by detecting  $(\text{CH}_3\text{OH})\text{Na}^+$ ,  $(\text{CH}_3\text{OH})_2\text{Na}^+$  and  $(\text{CH}_3\text{OH})_3\text{Na}^+$ , respectively. Although we apply mass-selective detection of ions to record the IR depletion spectra, this does not guarantee the spectral assignment of the neutral complex since ion fragmentation by loss of one or more methanol molecules could lead to the same absorption band being seen in spectra from different mass channels. However, mass selectivity does make it possible to establish the *minimum* number of methanol molecules in the complex (or complexes) contributing to a particular IR spectrum.

We can also use the dependence of the IR signal on the methanol pick-up pressure to help establish  $n$  and this was used previously to confirm the spectral assignments for  $\text{NaCl}(\text{H}_2\text{O})_n$ .<sup>5</sup> Figure 7 shows pick-up pressure (PUCP) data for  $\text{NaCl}(\text{CH}_3\text{OH})_n$ . Also shown are Poisson curves for different values of  $n$ , which should describe the probability of picking up  $n$  dopant molecules in the limit of negligible droplet shrinkage after pick-up. Unfortunately, the PUCP measurements for  $\text{NaCl}(\text{CH}_3\text{OH})_n$  are not as definitive as for  $\text{NaCl}(\text{H}_2\text{O})_n$  and there are two reasons for this. First, there are overlapping bands for different sized complexes, as will be evident by looking at Figures 2(a), (b) and (c), where peaks are seen at similar positions in different mass channels. Second, the relatively narrow OH stretching bands sit astride a broad underlying absorption feature, which we attribute to complexes with relatively large values of  $n$  ( $\geq 4$ ). This quasi-continuous absorption is very obvious in the  $(\text{CH}_3\text{OH})_2\text{Na}^+$  and  $(\text{CH}_3\text{OH})_3\text{Na}^+$  mass channels in Figure 2, but there is even a contribution in the  $(\text{CH}_3\text{OH})\text{Na}^+$  channel and this grows as the partial pressure of methanol is increased. We can partially offset the effect of the broad absorption envelope by estimating and subtracting its contribution from the intensities of the narrower peaks as the methanol

partial pressure is changed. However, the overlapping of the sharper bands restricts the information that can be extracted from PUCP data.

Before we attempt to make specific assignments, we note that the sharp bands in the OH stretching region, whose positions are summarized in Table 1, all lie between 3230 and 3360  $\text{cm}^{-1}$ . This is a relatively narrow range and the frequencies of these absorption bands are well to the red of the OH stretching band of the isolated methanol molecule.<sup>18</sup> This red shift is characteristic of the formation of ionic hydrogen bonds, which weaken the OH bonds and thereby lower the OH stretching frequencies. This effect has been seen previously in IR spectra of the anionic  $\text{Cl}^-(\text{CH}_3\text{OH})_n$  complexes, which have been studied in the gas phase by Lisy and co-workers.<sup>19,20</sup> Clearly there are some expected similarities between the interactions of methanol with  $\text{Cl}^-$  and  $\text{NaCl}$  given that the latter is a strongly ionic molecule, and so we compare key features of their spectra here. For  $\text{Cl}^-(\text{CH}_3\text{OH})_2$  two distinct structures were identified from the IR spectra: (1) one in which each methanol molecule is bound to  $\text{Cl}^-$  by an ionic hydrogen bond and (2) a ‘two-shell’ structure in which a methanol molecule binds to  $\text{Cl}^-$  by an IHB and then the second methanol molecule binds to the first by a normal hydrogen bond. The latter structure delivers a cooperatively *enhanced* IHB and results in an intense and hugely red-shifted band for this OH group, which appears at 2773  $\text{cm}^{-1}$ .<sup>20</sup> We see no OH stretching bands with anything like such large red shifts and so conclude that in small  $\text{NaCl}(\text{CH}_3\text{OH})_n$  clusters there is no hydrogen bonding between the methanol molecules. This distinction between  $\text{Cl}^-(\text{CH}_3\text{OH})_n$  and  $\text{NaCl}(\text{CH}_3\text{OH})_n$  most likely derives from the additional electrostatic stabilization provided by interaction between  $\text{Na}^+$  and the O atom on methanol when an IHB forms with the chloride ion in  $\text{NaCl}$  (for example see the global energy minimum structure for  $\text{NaCl}(\text{CH}_3\text{OH})$  in Figure 3). Structures with the maximum number of IHBs will be energetically favoured for small values of  $n$ .

We now attempt to make assignments for specific bands. We start by looking for the IR spectrum of the smallest complex, NaCl(CH<sub>3</sub>OH). Taking into account possible ion fragmentation, the spectrum of this complex might be observable as signal depletion in the Na<sup>+</sup> or (CH<sub>3</sub>OH)Na<sup>+</sup> mass channels. Previously we were able to record the IR spectrum of NaCl(H<sub>2</sub>O) by detecting Na<sup>+</sup>.<sup>5</sup> However, when H<sub>2</sub>O is replaced by CH<sub>3</sub>OH there are no OH stretching features when detecting Na<sup>+</sup> (see Supporting Information) and so we conclude that ionization of NaCl(CH<sub>3</sub>OH) in a helium droplet leads to ejection of Cl but not accompanied by CH<sub>3</sub>OH. Consequently, the IR spectrum of NaCl(CH<sub>3</sub>OH) must lie within the scan recorded by detecting (CH<sub>3</sub>OH)Na<sup>+</sup>, namely Figure 2(a). This spectrum shows two partly overlapping bands, one peaking at 3254 cm<sup>-1</sup> and the other at 3271 cm<sup>-1</sup>, with the former being marginally stronger. Of these two bands, that at 3254 cm<sup>-1</sup> has no exact counterpart in spectra from higher mass channels in Figure 2, although it does partly overlap with a peak whose maximum is at 3236 cm<sup>-1</sup> in the (CH<sub>3</sub>OH)<sub>2</sub>Na<sup>+</sup> channel. Since the bands are relatively broad, with full widths at half maximum  $\geq 15$  cm<sup>-1</sup>, an underlying contribution to the 3254 cm<sup>-1</sup> band from a larger complex is inevitable. The PUCP curve for this band in Figure 7 confirms this, showing a pressure-dependence that is more in keeping with  $n = 2$  than  $n = 1$ . Consequently, while we suspect that the peak at 3254 cm<sup>-1</sup> has a contribution from IR absorption by NaCl(CH<sub>3</sub>OH), this assignment must be seen as tentative. The other band seen in the (CH<sub>3</sub>OH)Na<sup>+</sup> mass channel, at 3271 cm<sup>-1</sup>, is partly coincident with a band seen in both the (CH<sub>3</sub>OH)<sub>2</sub>Na<sup>+</sup> and (CH<sub>3</sub>OH)<sub>3</sub>Na<sup>+</sup> mass channels, which peaks at 3278 cm<sup>-1</sup>. It is therefore possible that the 3271 cm<sup>-1</sup> band in the (CH<sub>3</sub>OH)Na<sup>+</sup> channel is entirely an absorption band of NaCl(CH<sub>3</sub>OH)<sub>2</sub> and/or a larger complex, which fragments on ionization.

Beneath the experimental spectrum in Figure 2(a) is a simulation of the IR spectrum derived from DFT calculations for the global minimum energy isomer for NaCl(CH<sub>3</sub>OH). If only this isomer is present in helium nanodroplets then only a single OH stretching band is

expected. The band assigned to NaCl(CH<sub>3</sub>OH) in the IR spectrum is red-shifted by  $\sim 430\text{ cm}^{-1}$  from the OH stretching band of the methanol monomer in superfluid helium,<sup>18</sup> implying a very significant weakening of the O-H bond when methanol forms a complex with NaCl. This is consistent with the formation of an ionic hydrogen bond (IHB) between the OH and the chloride ion. The corresponding red-shift for the anionic complex, (CH<sub>3</sub>OH)Cl<sup>-</sup>, in the gas phase is  $519\text{ cm}^{-1}$ .<sup>20</sup> The smaller red-shift for NaCl(CH<sub>3</sub>OH) when compared to the anion is reasonable for two reasons. First, the negative charge on the chloride ion in NaCl is expected to be smaller than for bare Cl<sup>-</sup>, making the IHB weaker. Second, electrostatic interactions between the Na and O atoms is also likely to modify the strength of the IHB. The experimental and DFT band positions in Figure 2(a) are in close agreement (the difference is  $10\text{ cm}^{-1}$ ), providing additional support for the assignment. Note that we can rule out contributions from other possible isomers shown in Figure 3 since, in addition to being much higher in energy, they do not have IHBs and therefore will have OH stretching bands at much higher frequencies than those seen in Figure 2 (see Supporting Information).

The DFT calculations predict a global minimum energy structure for NaCl(CH<sub>3</sub>OH)<sub>2</sub> in which each methanol molecule is independently bonded to the NaCl in a symmetrical configuration involving two IHBs. Consequently, symmetric and antisymmetric combinations of the two OH stretching vibrations will deliver two absorption bands. The sharing of Cl<sup>-</sup> among two IHBs leads to a net weakening of each individual IHB when compared to NaCl(CH<sub>3</sub>OH) because the negative charge is now shared between two IHBs. As a result, the O-H bonds strengthen and a smaller red-shift for the OH stretches of NaCl(CH<sub>3</sub>OH)<sub>2</sub> versus NaCl(CH<sub>3</sub>OH) is expected. The spectrum in Figure 2(b), recorded in the (CH<sub>3</sub>OH)<sub>2</sub>Na<sup>+</sup> mass channel, shows two prominent bands of almost equal intensity, one centered at  $3236\text{ cm}^{-1}$  and the other at  $3278\text{ cm}^{-1}$ . The band at  $3236\text{ cm}^{-1}$  has no counterpart in the spectrum recorded in the (CH<sub>3</sub>OH)<sub>3</sub>Na<sup>+</sup> mass channel and so we assign it to NaCl(CH<sub>3</sub>OH)<sub>2</sub>. This is supported by

the corresponding PUCP curve in Figure 7, which matches the Poisson curve for  $n = 2$  quite closely. The DFT calculations predict a splitting of  $26 \text{ cm}^{-1}$  between the antisymmetric and symmetric OH stretches for the lowest energy isomer of  $\text{NaCl}(\text{CH}_3\text{OH})_2$ . We therefore expect a second band at higher wavenumber and it is likely that the band peaking at  $3278 \text{ cm}^{-1}$  has a contribution from  $\text{NaCl}(\text{CH}_3\text{OH})_2$ . However, a band is also seen at a similar position in the  $(\text{CH}_3\text{OH})_3\text{Na}^+$  mass channel (see below) and so the  $3278 \text{ cm}^{-1}$  band in Figure 2(b) probably has contributions from both  $\text{NaCl}(\text{CH}_3\text{OH})_2$  and  $\text{NaCl}(\text{CH}_3\text{OH})_3$ . This seems to be supported by the PUCP data, which are somewhat scattered but fall between the Poisson curves for  $n = 2$  and 3. Given this assignment the splitting between the antisymmetric and symmetric OH stretching vibrations in  $\text{NaCl}(\text{CH}_3\text{OH})_2$  is *ca.*  $42 \text{ cm}^{-1}$ , which is larger than the  $26 \text{ cm}^{-1}$  predicted from the DFT calculations. The central position between these two bands is shifted to the blue of the single OH stretching band of  $\text{NaCl}(\text{CH}_3\text{OH})$ , as expected, but the shift is only  $+3 \text{ cm}^{-1}$  whereas the DFT calculations predict a value of  $41 \text{ cm}^{-1}$ . Other isomers, such as the next lowest energy isomer at  $2.9 \text{ kJ mol}^{-1}$  above the global minimum, do not offer a better match with experiment (see Supporting Information).

The strongest band in the  $(\text{CH}_3\text{OH})_3\text{Na}^+$  mass channel peaks at  $3278 \text{ cm}^{-1}$  and was mentioned above, since it overlaps with a band at a similar position in the  $(\text{CH}_3\text{OH})_2\text{Na}^+$  mass channel. This band is assigned to  $\text{NaCl}(\text{CH}_3\text{OH})_3$ , since there is no obviously sharp structure at this position above the broad absorption envelope in the spectrum in Figure 2(d) from the  $(\text{CH}_3\text{OH})_4\text{Na}^+$  mass channel. Of course it is possible that ionization of a particular isomer of  $\text{NaCl}(\text{CH}_3\text{OH})_4$  could generate  $(\text{CH}_3\text{OH})_3\text{Na}^+$  but this isomer-selective ion fragmentation seems unlikely. This is confirmed by the PUCP data, which most closely match the  $n = 3$  Poisson curve. The lowest energy isomer of  $\text{NaCl}(\text{CH}_3\text{OH})_3$  is expected to contain three equivalent IHBs, delivering two OH stretching bands because of the threefold rotational symmetry in this structure. Guided by the DFT predictions, the band at  $3278 \text{ cm}^{-1}$

is assigned to the degenerate antisymmetric OH stretch. Other weaker absorption features are seen to the blue (and are also seen in the  $(\text{CH}_3\text{OH})_2\text{Na}^+$  mass channel) at 3323 and 3349  $\text{cm}^{-1}$ . These peaks are too weak to extract useful PUCP data and so we offer speculative assignments. Given the predicted splitting of 36  $\text{cm}^{-1}$  we assign the band at 3323  $\text{cm}^{-1}$  to the symmetric OH stretch of  $\text{NaCl}(\text{CH}_3\text{OH})_3$ , although once again this gives an experimental splitting (45  $\text{cm}^{-1}$ ) which is significantly larger than the DFT prediction. We have no specific assignment for the weak band at 3349  $\text{cm}^{-1}$  (marked in Figure 2 with an asterisk) but speculate that it may arise from a higher energy isomer of  $\text{NaCl}(\text{CH}_3\text{OH})_3$  or possibly even from  $\text{NaCl}(\text{CH}_3\text{OH})_4$ .

There is a dramatic change in the IR spectra in going from detection of  $(\text{CH}_3\text{OH})_3\text{Na}^+$  to  $(\text{CH}_3\text{OH})_4\text{Na}^+$ , as seen by comparing Figures 2(c) and 2(d). The spectrum in Figure 2(d) can only come from a complex with at least four methanol molecules and shows only very broad absorption features in the OH stretching region, extending from roughly 3100 through to 3400  $\text{cm}^{-1}$ . A broad and largely structureless absorption in this region is also seen in the depletion spectrum recorded by detecting  $(\text{CH}_3\text{OH})_5\text{Na}^+$  (not shown here). We attribute the broadening in the OH stretching region to the presence of overlapping bands from multiple isomers for  $\text{NaCl}(\text{CH}_3\text{OH})_4$ , as well as possible contributions from larger complexes owing to ion fragmentation. In support of this statement, the DFT calculations have found seven local minima within 3  $\text{kJ mol}^{-1}$  of the global potential energy minimum of  $\text{NaCl}(\text{CH}_3\text{OH})_4$ , as illustrated in Figure 6. In Figure 2(d) we show the predicted IR contributions from each of these isomers. No attempt has been made to employ a Boltzmann weighting to the relative contributions of the various isomers as this may not apply here, given that rapid cooling by the helium can trap molecules in metastable structures. However, the simulation does show that contributions from multiple isomers would span the observed absorption range of 3200-3450  $\text{cm}^{-1}$  and is therefore a plausible explanation for the spectral broadening.

#### 4. *Assignment of IR spectra: CH stretching*

Clear bands are also seen from  $\text{NaCl}(\text{CH}_3\text{OH})_n$  complexes in the CH stretching region. The CH stretching bands in Figure 2 are particularly strong for the spectra derived by detecting lighter  $(\text{CH}_3\text{OH})_n\text{Na}^+$  ions but there is also a recognizable trace of CH structure in the spectrum recorded at  $m/z$  151 ( $(\text{CH}_3\text{OH})_4\text{Na}^+$ ), which can only come from complexes with  $n \geq 4$ . The CH absorptions consist of three prominent bands at roughly 2830, 2950 and 2975  $\text{cm}^{-1}$ , which are shifted a few  $\text{cm}^{-1}$  to the red of comparable bands in the isolated methanol molecule in liquid helium.<sup>19</sup> By analogy with free methanol these three bands can be assigned to the  $\nu_3$ ,  $\nu_9$  and  $\nu_2$  vibrations of the methanol units in  $\text{NaCl}(\text{CH}_3\text{OH})_n$ , respectively. The  $\nu_3$  mode is the symmetric CH stretch of the  $\text{CH}_3$  group, while  $\nu_9$  and  $\nu_2$  are both antisymmetric CH stretches. These mode descriptions are approximate, since multiple anharmonic couplings with overtone and combination states, such as  $2\nu_{10}$  and  $\nu_4 + \nu_{10}$ , are well known in this region.<sup>21</sup> Indeed a broad feature to the immediate red of the  $\nu_9$  band, which is most apparent in Figures 2(b) and (c), probably reflects this additional vibrational complexity.

The fact that there is no significant change in the CH stretching structure in Figure 2 as the mass channel is changed suggests that the methyl group has no role in the binding of NaCl to methanol. This is entirely consistent with the theoretical predictions for the global minima, where binding of  $\text{CH}_3\text{OH}$  is dominated by IHBs and where there is no involvement of the methyl group. However, the DFT calculations do not do a particularly good job at predicting the positions of the CH stretching bands, in part because the scaling factor chosen is optimum for the OH stretching modes. Also, the intensities of the CH stretching bands in the experimental spectra relative to the OH stretches are considerably higher than the DFT predictions, suggesting deficiencies in the particular DFT model employed here.

## Conclusions

Infrared spectra have been recorded for  $\text{NaCl}(\text{CH}_3\text{OH})_n$  complexes for the first time. Discrete vibrational bands are seen in the OH and CH stretching regions for  $n = 1-3$ . The positions of the OH stretching bands are consistent with formation of a dominant isomer in which the chloride ion undergoes an ionic hydrogen bond to the OH group in each methanol molecule. This contrasts with  $\text{Cl}^-(\text{CH}_3\text{OH})_n$  ions, where isomers with cooperatively enhanced ionic hydrogen bonds have been seen for  $n \geq 2$ .<sup>20</sup> For  $n \geq 4$  the discrete bands in the OH stretching region are replaced by broad absorption envelopes. This marked change in the spectra suggests that multiple isomers form for  $n \geq 4$  in the liquid helium environment.

## Acknowledgements

The authors are grateful to the Leverhulme Trust (RPG-2012-740) and the UK Engineering and Physical Sciences Research Council (GR/N002148/1) for grants in aid of this work. Support from the University of Nottingham for access to its High-Performance Computing facility and the Ministry of Higher Education and Scientific Research in Iraq for a PhD studentship for AMS are also gratefully acknowledged.

## References

1. Eisenberg, B. Ionic Interactions Are Everywhere. *Physiology* **2013**, *28*, 28-38.
2. Ault, B. S. Infrared spectra of argon matrix-isolated alkali halide salt/water complexes. *J. Am. Chem. Soc.* **1978**, *100*, 2426-2433.
3. Mizoguchi, A.; Ohshima, Y.; Endo, Y. Microscopic Hydration of the Sodium Chloride Ion Pair. *J. Am. Chem. Soc.* **2003**, *125*, 1716-1717.



4. Mizoguchi, A.; Ohshima, Y.; Endo, Y. The study for the incipient solvation process of NaCl in water: The observation of the  $\text{NaCl}-(\text{H}_2\text{O})_n$  ( $n = 1, 2, \text{ and } 3$ ) complexes using Fourier-transform microwave spectroscopy. *J. Chem. Phys.* **2011**, *135*, 064307.
5. Tandy, J.; Feng, C.; Boatwright, A.; Sarma, G.; Sadoon, A.; Shirley, A.; Das Neves Rodrigues, N.; Cunningham, E.; Yang, S.; Ellis, A. M. Infrared spectroscopy of salt-water complexes. *J. Chem. Phys.* **2016**, *144*, 121103.
6. Pinho, S. P.; Macedo, E. A. Solubility of NaCl, NaBr, and KCl in Water, Methanol, Ethanol, and their Mixed Solvents. *J. Chem. Eng. Data* **2005**, *50*, 29-32.
7. Li, M.; Constantinescu, D.; Wang, L.; Mohs, A.; Gmehling, J. Solubilities of NaCl, KCl, LiCl, and LiBr in Methanol, Ethanol, Acetone, and Mixed Solvents and Correlation Using the LIQUAC Model. *Ind. Eng. Chem. Res.* **2010**, *49*, 4981-4988.
8. Butler, J. A. V.; Thomson, D. W. The Behaviour of Electrolytes in Mixed Solvents. Part V. The Free Energy of Lithium Chloride in Water-Alcohol Mixtures and the Salting-Out of Alcohol. *Proc. Royal Soc. London, Series A* **1933**, *141*, 86-94.
9. Jungwirth, P.; Hofmeister Series of Ions: A Simple Theory of a Not So Simple Reality *J. Phys. Chem. Lett.* **2013**, *4*, 4258-4259.
10. Bowron, D. T.; Finney, J. L. Anion Bridges Drive Salting Out of a Simple Amphiphile from Aqueous Solution. *Phys. Rev. Lett.* **2002**, *89*, 215508.
11. Paschek, D.; Geiger, A.; Hervé, M. J.; Suter D., Adding salt to an aqueous solution of *t*-butanol: Is hydrophobic association enhanced or reduced? *J. Chem. Phys.* **2006**, *124*, 154508.
12. Shepperson, B.; Tandy, J.; Boatwright, A.; Feng, C.; Spence, D.; Shirley, A.; Yang, S.; Ellis, A. M. Electronic spectroscopy of toluene in helium nanodroplets: evidence for a long-lived excited state. *J. Phys. Chem. A* **2013**, *117*, 13591-13595.

13. Lester, J. E.; Somorjai, G. A. Studies of the Evaporation Mechanism of Sodium Chloride Single Crystals. *J. Chem. Phys.* **1968**, *49*, 2940-2949.
14. Shao, Y.; Gan, Z.; Epifanovsky, E.; Gilbert, A. T. B.; Wormit, M.; Kussmann, J.; Lange, A. W.; Behn, A.; Deng, J.; Feng, X.; et al., Advances in molecular quantum chemistry contained in the Q-Chem 4 program package. *Molec. Phys.* **2014**, *113*, 184-215.
15. Zhao, Y.; Truhlar, D. G. The M06 suite of density functionals for main group thermochemistry, thermochemical kinetics, noncovalent interactions, excited states, and transition elements: two new functionals and systematic testing of four M06-class functionals and 12 other functionals, *Theor. Chem. Acc.* **2008**, *120*, 215-241.
16. Scott, A. P.; Radom, L.; Harmonic Vibrational Frequencies: An Evaluation of Hartree–Fock, Møller–Plesset, Quadratic Configuration Interaction, Density Functional Theory, and Semiempirical Scale Factors, *J. Phys. Chem.* **1996**, *100*, 16502-16513.
17. Lin, C. Y.; Gilbert, A. T. B.; Gill, P. M. W. Calculating molecular vibrational spectra beyond the harmonic approximation, *Theor. Chem. Acc.* **2008**, *120*, 23-35.
18. Raston, P. L.; Douberly, G. E.; Jäger, W.; Single and double resonance spectroscopy of methanol embedded in superfluid helium nanodroplets. *J. Chem. Phys.* **2014**, *141*, 044301.
19. Cabarcos, O. M.; Weinheimer, C. J.; Martínez, T. J.; Lisy, J. M. The solvation of chloride by methanol—surface versus interior cluster ion states. *J. Chem. Phys.* **1999**, *110*, 9516-9526.
20. Beck, J. P.; Lisy, J. M. Cooperatively Enhanced Ionic Hydrogen Bonds in  $\text{Cl}^-(\text{CH}_3\text{OH})_{1-3}\text{Ar}$  Clusters. *J. Phys. Chem. A* **2010**, *114*, 10011-10015.

21. Gruenloh, C. J.; Florio, G. M.; Carney, J. R.; Hagemester, F. C.; Zwieter, T. S. C-H Stretch Modes as a Probe of H-Bonding in Methanol-Containing Clusters. *J. Phys. Chem. A* **1999**, *103*, 496-502.

**Table 1.** Positions and assignments of OH stretching bands for  $\text{NaCl}(\text{CH}_3\text{OH})_n$  for  $n = 1-3$ .

Band position	Assigned carrier
3236	$\text{NaCl}(\text{CH}_3\text{OH})_2$
3254	$\text{NaCl}(\text{CH}_3\text{OH})$
3278	$\text{NaCl}(\text{CH}_3\text{OH})_2 + \text{NaCl}(\text{CH}_3\text{OH})_3$
3323	$\text{NaCl}(\text{CH}_3\text{OH})_3?$
3344	$\text{NaCl}(\text{CH}_3\text{OH})_3?$

## Figure captions

1. Mass spectrum from the NaCl/CH<sub>3</sub>OH system obtained using an electron energy of 70 eV. Three series of ions are seen in this spectrum. Although not labelled in this figure, peaks from He<sub>*n*</sub><sup>+</sup> cluster ions are particularly evident on the low mass side of the spectrum. The two labelled ion series correspond to (CH<sub>3</sub>OH)<sub>*m*</sub>H<sup>+</sup> and (CH<sub>3</sub>OH)<sub>*m*</sub>Na<sup>+</sup>, where the former derive from helium droplets containing only methanol molecules and the latter derive from NaCl(CH<sub>3</sub>OH)<sub>*n*</sub> complexes.
2. Infrared spectra of NaCl(CH<sub>3</sub>OH)<sub>*n*</sub> recorded by monitoring ion signals at (a) *m/z* 55 ((CH<sub>3</sub>OH)Na<sup>+</sup>) (b) *m/z* 87 ((CH<sub>3</sub>OH)<sub>2</sub>Na<sup>+</sup>), (c) *m/z* 119 ((CH<sub>3</sub>OH)<sub>3</sub>Na<sup>+</sup>) and (d) *m/z* 151 ((CH<sub>3</sub>OH)<sub>4</sub>Na<sup>+</sup>). Also shown beneath the spectra in (a), (b) and (c) are the predicted IR spectra for the global minimum energy structures of *n* = 1-3, respectively, derived from DFT calculations. The asterisked peak in (b) and (c) is unassigned, as discussed in the main text. Beneath the spectrum in (d) we show the predicted IR bands for the *n* = 4 complex for the 8 lowest energy structures, which all lie within 3 kJ mol<sup>-1</sup> of the global minimum. The different colours represent different isomers and their intensities have not been weighted by any assumed abundance distribution (see main text for further details).
3. Calculated equilibrium structures for NaCl(CH<sub>3</sub>OH) along with their energies (not corrected for zero point energy) in kJ mol<sup>-1</sup> relative to the global potential energy minimum.

4. Calculated equilibrium structures for  $\text{NaCl}(\text{CH}_3\text{OH})_2$  along with their energies (not corrected for zero point energy) in  $\text{kJ mol}^{-1}$  relative to the global potential energy minimum.
5. Calculated equilibrium structures for  $\text{NaCl}(\text{CH}_3\text{OH})_3$  along with their energies (not corrected for zero point energy) in  $\text{kJ mol}^{-1}$  relative to the global potential energy minimum. For the global minimum structure the NaCl has been oriented with the Cl atom above the Na atom so as to show the trigonal ( $C_3$  rotational) symmetry about the Na-Cl bond axis.
6. Calculated equilibrium structures for  $\text{NaCl}(\text{CH}_3\text{OH})_4$  along with their energies (not corrected for zero point energy) in  $\text{kJ mol}^{-1}$  relative to the global potential energy minimum.
7. Dependence of the intensities of specific IR absorption bands, detected in the  $m/z$  55 ( $(\text{CH}_3\text{OH})\text{Na}^+$ ),  $m/z$  87 ( $(\text{CH}_3\text{OH})_2\text{Na}^+$ ) and  $m/z$  119 ( $(\text{CH}_3\text{OH})_3\text{Na}^+$ ) mass channels, on the partial pressure of methanol in the second pick-up cell. Also shown are the calculated Poisson curves for the pick-up of one (black), two (blue) and three (red) methanol molecules.

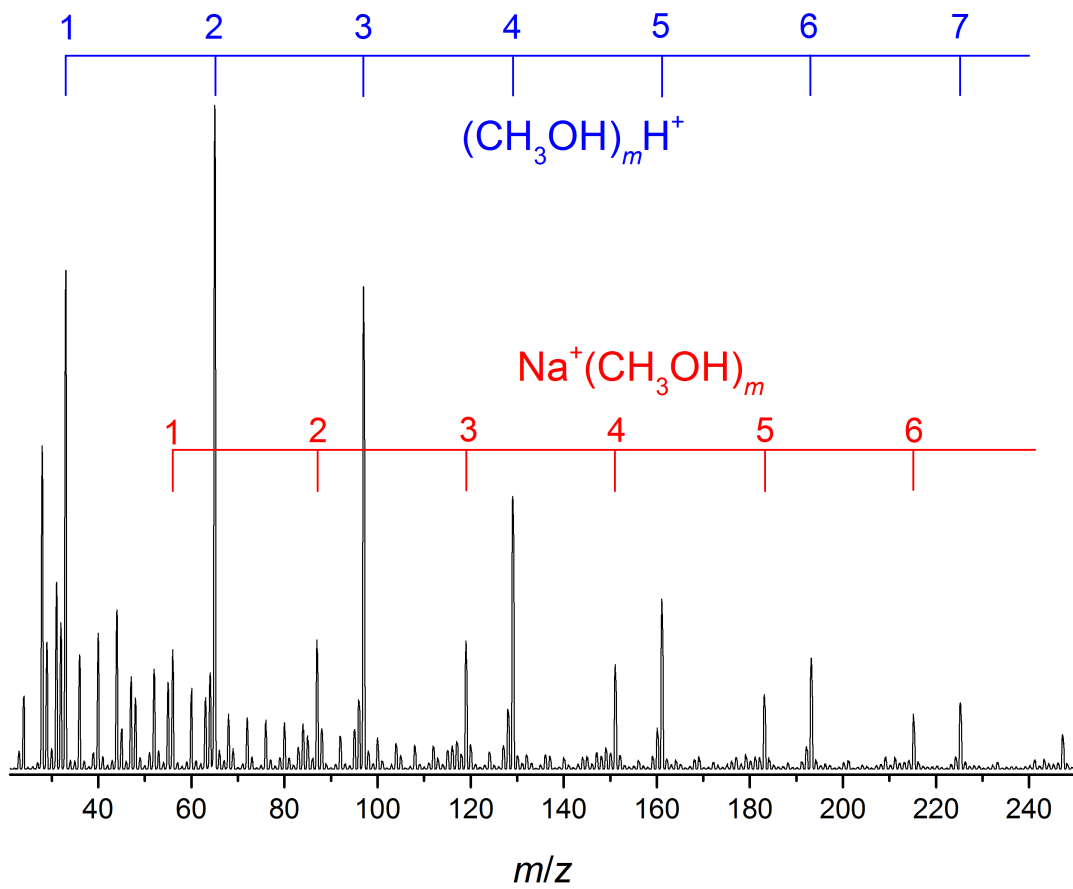


Figure 1

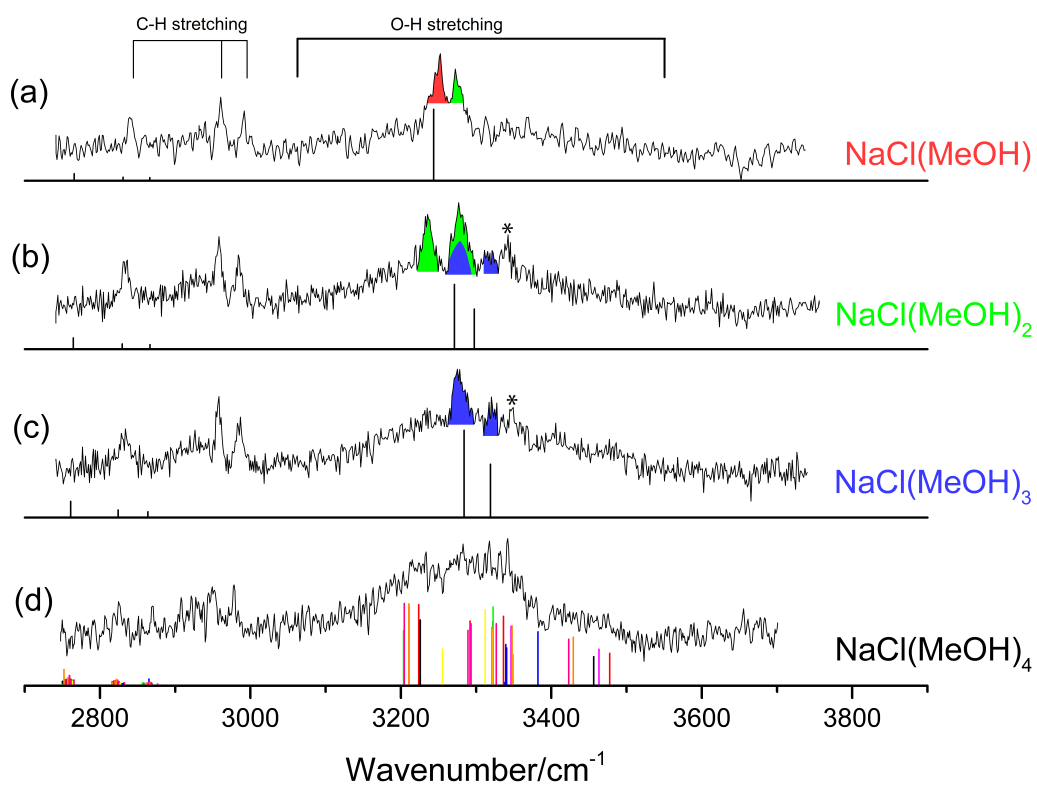


Figure 2



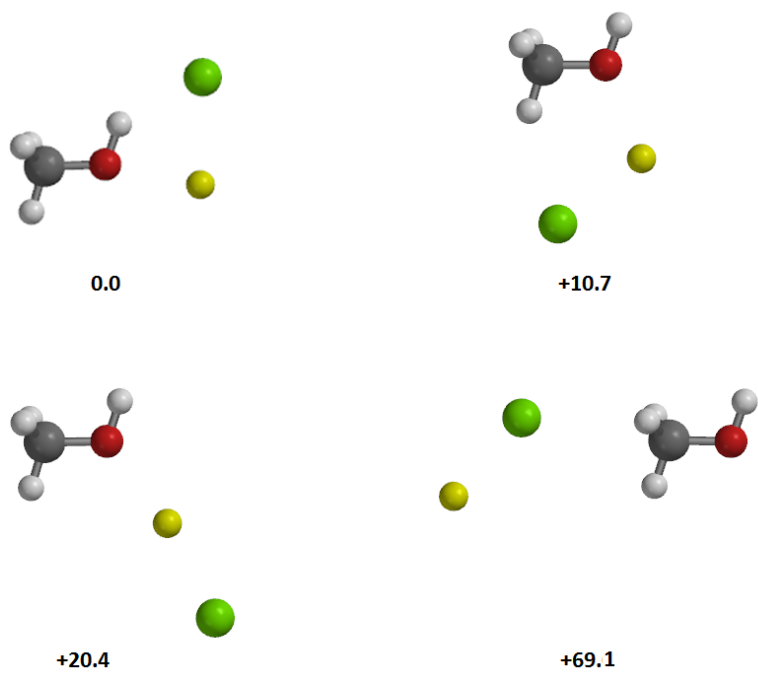


Figure 3

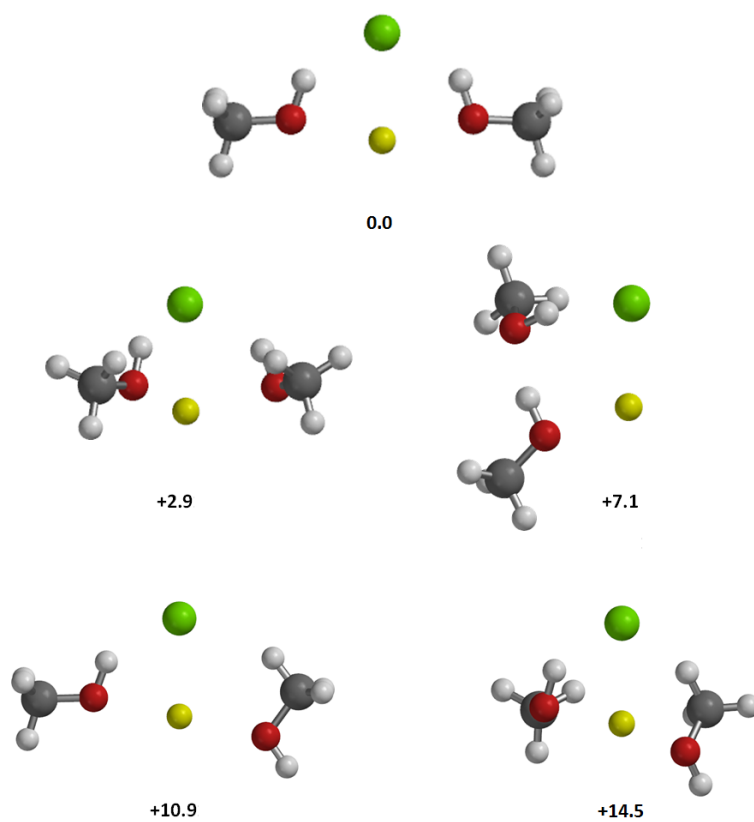


Figure 4

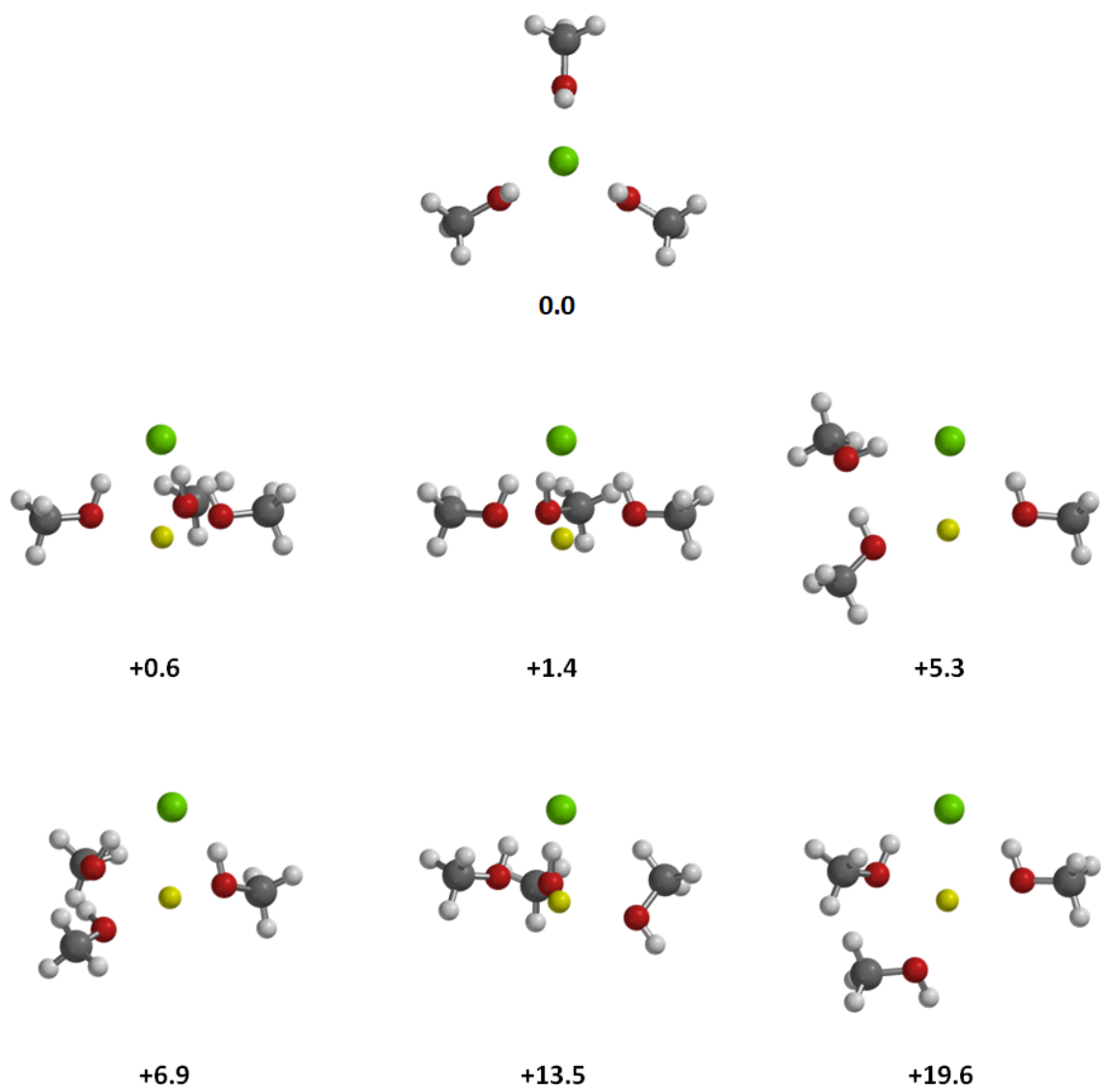


Figure 5

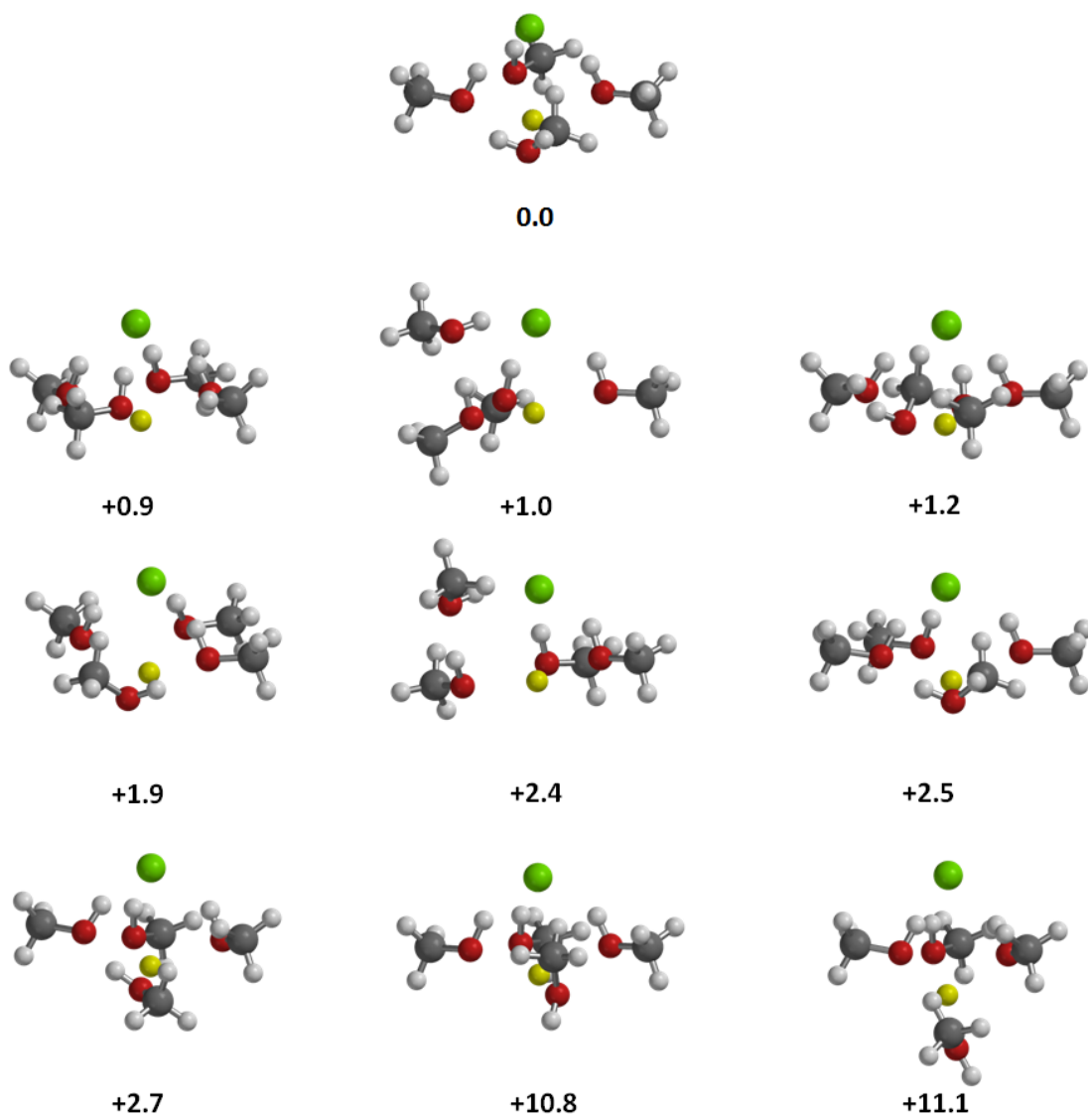


Figure 6

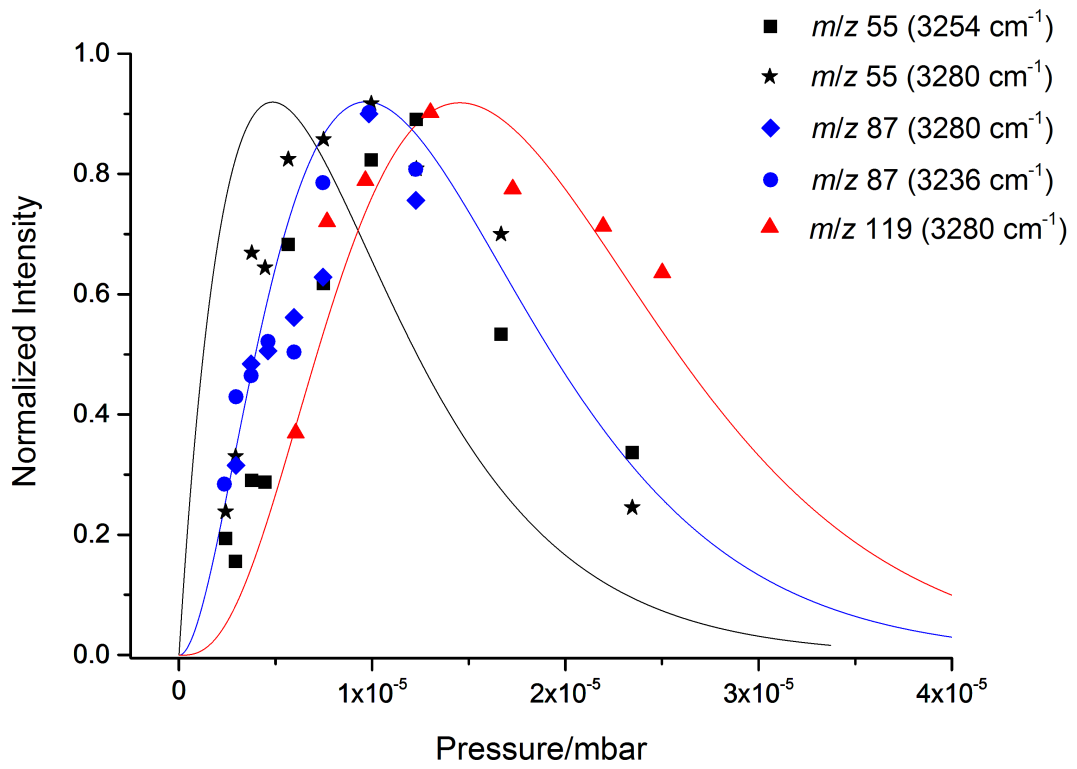


Figure 7